THE EUROPEAN
PHYSICAL JOURNAL C

Replica wormhole as a vacuum-to-vacuum transition

Yang An[1], **Peng Cheng**[2,3,a]

[1] Institute for Theoretical Physics and Cosmology, Zhejiang University of Technology, Hangzhou 310014, China
[2] Center for Joint Quantum Studies and Department of Physics, Tianjin University, Tianjin 300350, China
[3] Institute for Theoretical Physics, University of Amsterdam, 1090 GL Amsterdam, The Netherlands

Abstract The recent developments related to the black hole information paradox have brought us a confusing object: the replica wormhole. We are trying to better understand the object from the viewpoint of the thermo-mixed double and spontaneous symmetry breaking. In this paper, we show that the replica wormhole can be regarded as a transition between different degenerate vacua, and the corresponding gravitational partition function should be controlled by the manifold of the degenerate vacua. We also check the wormhole partition function in two-dimensional Jackiw–Teitelboim gravity and show that the wormhole saddle is indeed controlled by the dimension of the degenerate vacua. Moreover, it is suggested that the replica wormhole geometries connecting different vacua can be related to the measurement process of soft hair that compares different vacuum configurations.

1 Introduction

The black hole information paradox (BHIP) is a longstanding problem regarding the evolution of black hole systems, and we have seen exciting progress [1–7] in recent years. The Page cure [8,9] was derived from the quantum extremal surface prescription [10–16], and extra "island" contribution to the radiation entropy was the key ingredient for deriving the Page cure. When using the replica trick and Euclidean path integral to derive the island rule, the authors of [5,6] have found *replica wormhole* saddles which play a vital role in getting the Page curve.

Then, the most crucial question to ask is: how should we understand the replica wormhole? The replica ansatz [17,18] provided a way of understanding the replica wormhole by relating the n-fold wormhole and the thermo-mixed double state. In this paper, we will use a similar idea and show that the replica wormhole can be understood as a transition between different degenerate vacua.

Such ideas are well-motivated because it is natural to relate the wormhole saddle that decreases the radiation entropy and measurement process in soft BHIP story [19–21]. In QFT, the spontaneous symmetry breaking (SSB) of the global symmetry forms superselection sectors of Hilbert space, and no renormalizable operator can move the system between different sectors. However, as told by Hawking-Perry-Strominger (HPS) [22,23], there are infinite degenerate vacua at null boundaries because of the SSB of large gauge symmetry, and no superselection sector is formed (related properties at black hole horizon were analyzed in [24,25]). The degenerate vacua are labeled by local functions, such as $f(z_A)$ on the celestial sphere. It was suggested in the soft BHIP [19–21] that measurement processes that compare different functions $f(z_A)$ can decrease the entropy of a black hole system. The Hawking radiation process can increase the entropy by producing new radiations, while the soft hair measurement process can decrease the entropy by comparing different fs. The competition between the Hawking radiation and measurement process gives rise to the Page curve consistent with unitary evolution [20]. The argument shown in [19–21] is similar to the competition between connected and disconnected geometries shown in [5,6]. The disconnected "Hawking saddles" increase the entropy of the radiation and the black hole, while the connected "wormhole saddles" decrease the corresponding entropy. The aim of the study is to find a clear connection between the recent developments on Euclidean gravitational path integral and the soft BHIP story.

We explicitly show the relation between the replica wormhole and degenerate vacua in this paper. By a careful study of the thermo-mixed double and wormhole saddle, we show there can be different vacua on different boundaries of the wormhole saddle as opposed to the black hole partition function. Moreover, the wormhole partition function should be

---
[a] e-mail: p.cheng.nl@outlook.com (corresponding author)

proportional to the number of possible vacua and the replica wormhole geometry in calculating the radiation entropy should be regarded as a process that decreases the entropy. We then check the partition function of the wormhole saddle in two-dimensional Jackiw–Teitelboim (JT) gravity, which serves as evidence for the proposal.

In this paper, we explore how should we understand replica wormholes. The paper is organized as follows. In Sect. 2, we offer a basic overview of how the replica wormhole arises. Then, Sect. 3 provides the argument on how to treat the replica wormholes as a transition from different degenerate vacua. Section 4 checks the above proposal in two-dimensional JT gravity. We summarize the paper and discuss further issues in Sect. 5. The Appendix A reviews the basic concepts of the Euclidean path integral and black hole thermodynamics.

2 Replica wormholes

In this section, following [5], we will see how the replica wormhole makes its appearance in the argument of the BHIP. The basics of the Euclidean path integral are reviewed in Appendix A. We are going to use $|\Psi\rangle$ to denote the pure system composing a black hole and radiation. Then we can trace out the black hole system to calculate the fine-grained entropy of the radiation. The state $|\Psi\rangle$ can be expressed as

$$|\Psi\rangle = \frac{1}{\sqrt{kZ_1}} \sum_{i=1}^{k} |\psi_i\rangle_B |i\rangle_R, \tag{1}$$

where $|\psi_i\rangle_B$ denotes the black hole states, $|i\rangle_R$ denotes radiation, and i labels the entanglement between the radiation and black hole. The normalization factor is chosen such that under

$$\langle\psi_i|\psi_j\rangle_B = \delta_{ij} Z_1, \quad \langle i|j\rangle_R = \delta_{ij}. \tag{2}$$
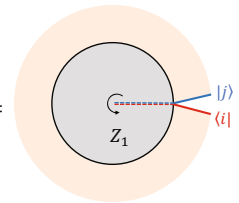
the amplitude

$$\sum_{\Psi} \langle\Psi|\Psi\rangle = 1. \tag{3}$$

The density matrix of radiation can be obtained by tracing out the black hole system

$$\rho_R = \sum_m \langle\psi_m|\Psi\rangle \langle\Psi|\psi_m\rangle = \frac{1}{k} \sum_{i,j} |i\rangle_R \langle j| \langle\psi_j|\psi_i\rangle_B \tag{4}$$

which can be illustrated as

$$\rho_R = \qquad \qquad . \tag{5}$$

The density matrix is represented in the same way as we described in the previous section.

Instead of directly using the density matrix to calculate the entropy, one can look at purity $\mathrm{tr}[\rho_R^2]$, where we have

$$\mathrm{tr}[\rho_R^2]$$
$$= \frac{1}{k^2 Z_1^2} \sum_l \sum_{i,j} \sum_{m,n} \langle l|i\rangle \langle j| \langle\psi_j|\psi_i\rangle |m\rangle \langle n| \langle\psi_n|\psi_m\rangle |l\rangle$$
$$= \frac{1}{k^2 Z_1^2} \sum_{i,j} \left[\langle\psi_i|\psi_j\rangle\langle\psi_j|\psi_i\rangle \right] + \frac{1}{k^2 Z_1^2} \sum_{i,j} \left[\langle\psi_i, \psi_j|\psi_i, \psi_j\rangle \right]$$
$$= \frac{kZ_1^2 + k^2 Z_2}{k^2 Z_1^2}, \tag{6}$$

where Z_1 is the geometry described in equation (5), and Z_2 represents the two-fold replica wormhole shown in Fig. 1. Now, the purity can be expressed as

$$\mathrm{tr}[\rho_R^2] = \frac{kZ_1^2 + k^2 Z_2}{k^2 Z_1^2} = \frac{1}{k} + \frac{Z_2}{Z_1^2}. \tag{7}$$

The calculation shown in (6) is explicitly illustrated in Figs. 1 and 2.

The two-fold wormhole shown in Fig. 1 can be ironed to a flat version

$$\qquad \qquad , \tag{8}$$

where we only show the gravitational region (grey region) of Fig. 1. The wormhole geometry can be recovered by gluing the dashed lines with the same color together in (8). The above geometry can be easily extended to n-fold replica wormholes, which can be used to calculate the n-th Renyi entropy $\mathrm{tr}[\rho_R^n]$. The von Neumann entropy is essentially determined by $\mathrm{tr}[\rho_R^n]$ when analytically continued to $n = 1$. There are more different saddles for the n-th Renyi entropy: fully connected, fully disconnected, and other partially connected saddles. The saddles with more disconnected components dominate at the early stage when k is relatively small. And the connected geometries play a more important role
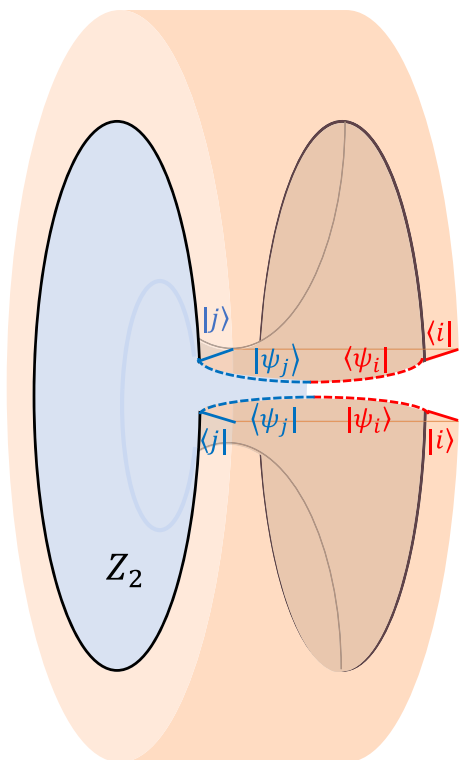
Fig. 1 Replica wormhole saddle in calculating the purity of radiation (6). The picture is a diagrammatic representation of $\sum_{i,j} \langle \psi_i, \psi_j | \psi_i, \psi_j \rangle$. There is a wormhole geometry, and the final result is $\sum_{i,j} \langle \psi_i, \psi_j | \psi_i, \psi_j \rangle = k^2 Z_2$. Note that the * symbol representing the CPT transformation is not explicitly shown in the figure
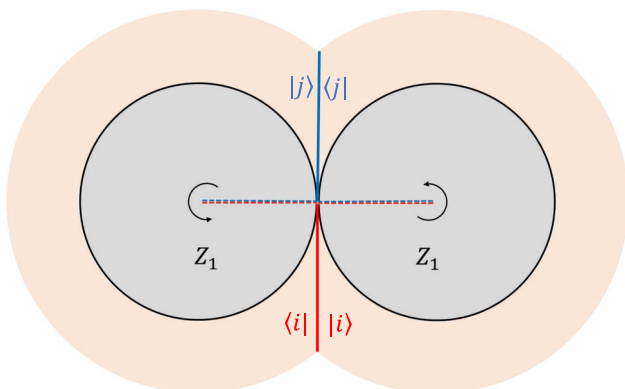

Fig. 2 Hawking saddle in calculating the purity of radiation (6). The corresponding result is $\sum_{i,j} \langle \psi_i | \psi_j \rangle \langle \psi_j | \psi_i \rangle = k Z_1^2$

at the late stage of evaporation. We can add all the different saddles together, and the transitions between different saddles lead to an entropy of radiation that is consistent with the unitarity [5,6].

3 Transition between different vacua

Let us think about what the replica wormhole saddle, shown in Fig. 1, means in gravity. As shown in Appendix A, the Euclidean black hole partition function can be got by tracing the thermofield double (TFD) state,

$$Z_{BH} = \sum_{\phi} \qquad = \qquad . \qquad (9)$$

which is a gravitational generalization of the Rindler partition function getting from Eq. (50). Looking at the replica wormhole, we find that we have lost our favorite TFD state shown in (50). If one insists that the density matrix of the replica wormhole should also be got from tracing over some TFD-like state, we can express the wormhole density matrix ρ_{WH}, with "WH" representing wormhole, as

$$\rho_{\text{WH}} = \sum_{\phi_1, \phi_2} \qquad = \qquad . \qquad (10)$$

Now, assuming the wormhole density matrix is obtained from some reduced density matrix, we have got the density matrix of the *thermo-mixed double* (TMD) [17,18,26,27], which can be illustrated as

$$\rho_{\text{TMD}} = \qquad . \qquad (11)$$

ρ_{TMD} is the flat version of the up or down part of (10), and the connected region in the middle of (11) can be regarded as the "island". The TMD density can be called "Janus Pacman" to distinguish the Pacman figure shown in (48). The TMD and TFD are supposed to give out the same density matrix when tracing out the left part L
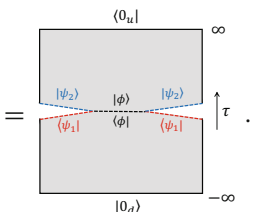
$$\rho_{BH} = \text{tr}_L(\rho_{\text{TMD}}) = \text{tr}_L(\rho_{\text{TFD}}), \qquad (12)$$

whose von Neumann entropy is the Bekenstein-Hawking entropy S_{BH}.[1]

Equipped with the TMD interpretation, let us look at what the replica wormhole means now. As discussed in Appendix A, the TFD state can be defined as a state evolved from the vacuum at $\tau = -\infty$. Here, by the same logic, we can also define the TMD as a state evolved from the vacuum. The vacuum evolved from $\tau = -\infty$ is denoted as $|0_d\rangle$ and the one from $\tau = \infty$ as $|0_u\rangle$. The subscripts u and d mark different possible vacua.

Those different vacua can be identified by trace operation. In (4), the trace over the gravity part $|\psi_i\rangle_B$ forces the vacuum to be identical, which can be seen from the closed black circle shown in Eq. (5). For the same reason, when the boundaries representing $|0_u\rangle$ and $|0_d\rangle$ are connected with each other, we have a unified vacuum, so putting an extra label on the vacuum state has no influence on the final result because of the trace operation. In the case of calculating the purity, the situation is exactly shown in Fig. 2, where the black line forms a closed circle in the Hawking saddle. So in the Hawking saddle, $|0_u\rangle$ and $|0_d\rangle$ are identified by the trace operation, and thus we have a unified vacuum, which is consistent with our usual understanding of quantum field theory with a given Hamiltonian. However, the situation is completely different for the replica wormhole saddle shown in Fig. 1. As can be seen from Fig. 1, the black lines representing $|0_u\rangle$ and $|0_d\rangle$ form two different circles, and no trace operation forces them to be identical. In principle, there can be different degenerate vacua, and that is the part where the different subscripts on $|0\rangle$ start to play an important role in the follow-up discussions. We leave the physical interpretation of degenerate vacua in the discussion section.

Now, we come to the key observation regarding the meaning of the replica wormhole. For the flat case corresponding to the Minkowski and Rindler spacetime, the TMD density matrix can be represented as

$$\langle \psi_1 | \rho_{\text{TMD}} | \psi_2 \rangle = \sum_{\phi} \langle \phi | \langle \psi_1 | 0_d \rangle \langle 0_u | \psi_2 \rangle | \phi \rangle$$

$$= \qquad (14)$$

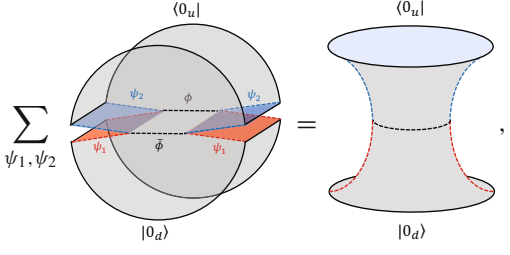And, the purity of the TMD density matrix can be further expressed as

$$
\begin{aligned}
&\text{tr}[\rho_{\text{TMD}}^2] \\
&= \sum_{\phi, \bar{\phi}} \sum_{\psi_1, \psi_2} \langle \psi_1 | \langle \phi | 0_d \rangle \langle 0_u | \phi \rangle | \psi_2 \rangle \\
&\quad \times \left[\langle \psi_1 | \langle \bar{\phi} | 0_d \rangle \langle \bar{\phi} | 0_u \rangle | \psi_2 \rangle \right]^* \\
&= \langle 0_u |^* \langle 0_u | 0_d \rangle | 0_d \rangle^*.
\end{aligned}
\qquad (15)
$$

Note that the above purity $\text{tr}[\rho_{\text{TMD}}^2]$ can only see the vacua because the system is evolved from the past infinity to future infinity. The excitation modes can not be seen due to the infinite distance between the two-time slices, which was elaborated in (41) for the disk case.

In order to see the gravitational effects in the bulk, we can imagine the down vacuum from the past infinity evolves to a finite time slice $\tau = -d/2$ and starts to feel the gravity. Then the system evolves to time slice $\tau = d/2$. After that gravity disappears and the system evolves to future infinity. This means that gravity is confined in a region between time slices $\tau = -d/2$ and $\tau = d/2$. Suppose the gravitational Hamiltonian is denoted as $\mathcal{H}$, one need to multiply the purity shown in (15) by

$$Z_{\text{gravity}} = \langle 0_d | e^{-\int_{-d/2}^{d/2} \mathcal{H} \, d\tau} | 0_d \rangle. \qquad (16)$$

Diagrammatically, the purity can be illustrated as gluing two copies of (14) together

$$\text{tr}[\rho_{\text{TMD}}^2] = \sum_{\psi_1, \psi_2}$$ $$=$$

$$(17)$$

which can be regarded as the inverse process of (10).

Comparing Eqs. (15) and (17), we can conclude that the two-fold replica wormhole should be proportional to the transition amplitude between the up and down vacua

$$Z_2 \propto \langle 0_u |^* \langle 0_u | 0_d \rangle | 0_d \rangle^* \times Z_{\text{gravity}}. \qquad (18)$$

Here, we have chosen to project the Hamiltonian onto a specific vacuum. The transition amplitude should always be proportional to the volume of degenerate vacua. Nevertheless, the point here is that the effect of the transition between different vacua should be included in Z_2. Here we use $\propto$ because the renormalization factor shown in (13) is not included.

Now, we can see that the replica wormhole also counts the transition from different vacua evolved from $\tau = -\infty$ to $\tau = \infty$. It is more clear that, as shown in (17), the state at $\tau = -\infty$ and $\tau = \infty$ are not necessarily the same because of the independent circles, which is different from the Hawking saddle where the up and down circles are connected because of trace operation. The allowance for different vacua to exist is suggested to understand lots of interesting physics related to wormholes like the factorization puzzle [28–30] and the black hole information paradox [21,31,32]. The conclusion can be easily generalized to n-fold replica wormholes, which can be regarded as transitions between more different vacua.

We would like to end this section with some comments on SSB and vacuum degeneracy. For a complex scalar field theory with Mexican hat potential, the vacuum degeneracy comes from the SSB of the global $U(1)$ symmetry. The minimum of the potential is characterized by a compact parameter ρ. Let us suppose the vacuum is chosen at a specific value $|\rho_0\rangle$ and there is a possible generator Q_θ that acts on the vacuum state and changes the value of ρ. The generator can be written as

$$e^{i Q_\theta} \, |\rho_0\rangle \sim |\rho_0 + \theta\rangle. \tag{19}$$

The generator Q_θ moves the QFT from one vacuum to a new one. However, the operator Q_θ is not in the Hilbert space because it is not normalizable. To see this physically, we can suppose the original vacuum is $|\rho_0\rangle$, and we want to change the global vacuum to a different one $|\rho_1\rangle$. We can start to change it with a bubble of local degrees of freedom with vacuum $|\rho_1\rangle$. There is a non-zero gradient of the scalar field on the edge, and the energy needed to flip the vacuum is proportional to the bubble area. Then it needs infinite energy to move all the local degrees of freedom from vacuum $|\rho_0\rangle$ to vacuum $|\rho_1\rangle$. So in QFT, superselection sectors are formed, and a specific vacuum is chosen.

However, there are two possible exceptions, where superselection sectors are not formed. The first one is low-dimension cases. In two dimensions, the area of the bubble is a point, and no superselection sector is formed. That is why we can twist left and right single trumpets for wormhole geometries in two-dimensional JT gravity. The second one is vacuum degeneracy due to the SSB of the large gauge (or diffeomorphism) symmetry. As opposed to the global case, the operators that move the theory between different vacua are not non-renormalizable operators. This is because would-be gauge symmetries are labeled by local functions, the SSB of which does not need to occur simultaneously everywhere.

As shown by HPS, there are infinite degenerate vacua at null boundaries because of the SSB of large gauge symmetry, and no superselection sector is formed. We can relate the vacuum degeneracy with the wormhole geometry, and the two-fold wormhole can be thought of as a transition between

different soft-hair-generated vacua. The replica wormhole can be regarded as the process comparing the would-be gauge parameter at the two boundaries, thus can decrease the entropy of the black hole and radiation.

4 Two-dimensional JT gravity

Let us check if the above proposal makes sense in the two-dimensional Euclidean JT gravity. In this calculable low-dimensional quantum gravity theory, we can check the property of the wormhole geometry.

The action of JT gravity can be written as

$$I_{JT}[g, \Phi] = -S_0 \chi - \frac{1}{16\pi G_N} \int_{\mathcal{M}} \sqrt{|g|} \Phi (R + 2)$$
$$- \frac{1}{8\pi G_N} \oint_{\partial \mathcal{M}} \sqrt{|g|} \Phi (K - 1), \tag{20}$$

with constant S_0 and Euler characteristic χ. With boundary condition

$$h_{tt}\big|_{\partial \mathcal{M}} = \frac{1}{\varepsilon^2}, \quad \Phi\big|_{\partial \mathcal{M}} = \frac{\Phi_b}{\varepsilon}, \tag{21}$$

the boundary action can be written as

$$I_{bdy}[F] = -C \int d\tau \{F, \tau\}, \quad C = \frac{\Phi_b}{16\pi G_N}. \tag{22}$$

We have $\varepsilon \to 0$ near the boundary, and $\{F, \tau\}$ is the Schwarzian derivative. In the black hole frame, we have

$$F(\tau) = \tan \frac{\pi}{\beta} f \tau. \tag{23}$$

The new variable $f(\tau)$ can be interpreted as a time reparametrization of the boundary thermal circle, with properties

$$f(\tau + \beta) = f(\tau) + \beta, \quad f'(\tau) \geq 0. \tag{24}$$

The bulk geometry is fixed to $R + 2 = 0$, so the boundary theory and $f(\tau)$ are the main object people usually care about in boundary theory. The boundary partition function, or the bulk disk partition function, can be calculated perturbatively. It was shown by Stanford and Witten [33] that the Schwarzian theory is one-loop exact using fermionic localization. The bulk black hole partition function can be written as (see [34] for review)

$$Z_1(\beta) = \frac{1}{4\pi^2} \left(\frac{2\pi C}{\beta} \right)^{3/2} e^{S_0 + \frac{2\pi^2 C}{\beta}} \tag{25}$$
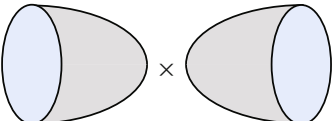
Let us consider gravitational partition function with n boundaries

$$Z(\beta_1, \beta_2, \ldots, \beta_n). \tag{26}$$

The partition function includes all possible topologies of the spacetime, and can be decomposed by Euler characteristic χ, i.e.

$$Z(\beta_1, \beta_2, \ldots, \beta_n) = \sum_g e^{S_0(2-2g-n)} \times Z_{g,n}(\beta_1, \beta_2, \ldots, \beta_n). \tag{27}$$

$Z_{0,2}(\beta_1, \beta_2)$ is what we care about in this paper, so let us see what this partition function is in JT gravity. We end up with two parts: disconnected and connected geometries. For disconnected disks, the partition function is
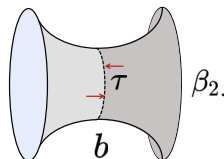
$$Z_1(\beta_1)Z_1(\beta_2) = \tag{28}$$

For connected geometry, we can glue two disk geometries with insertions of defects that breaks $PSL(2, R)$ to $U(1)$, which are called single trumpets. The partition function of the single trumpet is also one-loop exact and can be evaluated as

$$Z_{\text{trumpet}}(\beta) = \frac{1}{2\pi}\sqrt{\frac{2\pi C}{\beta}}e^{-\frac{C}{2\beta}b^2} \tag{29}$$

The remaining $U(1)$ is characterized by the twist parameter τ, and b is the length of the geodesic at the middle of the geometry

$$\tag{30}$$

The wormhole partition function should be an integral over the twist parameter τ, with $\int_0^b d\tau = b$. This is because (29) is independent of τ. Then, one can integrate all possible b to count all of the on-shell effects[2]

$$Z_{0,2}(\beta_1, \beta_2) = \int_0^\infty Z_{\text{trumpet}}(\beta_1)Z_{\text{trumpet}}(\beta_2)\, b\, db. \tag{31}$$

Note that we expect the wormhole geometry as a saddle of the path integral, while here the integral is over all possible

quantum configurations. Is there a "stable" wormhole saddle in the above integral? From (29), because b is pushed to zero in the exponential. But if we include the twist parameter and extremize the integrand, there is a stable value of b.[3] Solving

$$\partial_b[Z_{\text{trumpet}}(\beta_1)Z_{\text{trumpet}}(\beta_2)\, b] = 0, \tag{32}$$

one finds the solution

$$\bar{b} = \frac{\sqrt{\beta_1\beta_2}}{\sqrt{C(\beta_1 + \beta_2)}}. \tag{33}$$

The corresponding partition function can be written as

$$\bar{Z}_{0,2}(\beta_1, \beta_2) = \bar{b} \times \frac{C}{2\pi\sqrt{e\beta_1\beta_2}}. \tag{34}$$

$\bar{b}$ is the length of the twist parameter τ, that lables the $U(1)$ circle, as discussed in this section.

So, the JT calculation can be regarded as evidence of what we discussed in the previous section, shown in (18). The wormhole partition function is proportional to the number of vacua generated by the symmetry of the geometry.

5 Conclusion and discussion

In this paper, we address the question of how to understand the replica wormhole. When deriving the island rule from the Euclidean path integral, the replica wormhole saddle naturally arises and plays a vital role in the post-Page time. The replica wormhole connecting different replicas in the replica trick is a confusing object, and it is important to better understand the physical meaning of those wormhole geometries.

We have shown that the replica wormhole should be regarded as a transition between different degenerate vacua. More specifically, all the possible vacua in the Hawking saddle are identified because of the trace operation shown in Fig. 2, but the situation is different for the replica wormhole saddle in Fig. 1. There can be different vacua represented by the left and right black circles, and the purity of the TMD density matrix is shown to be proportional to the transition between two different vacua, which is illustrated in Eqs. 15 and 17. The same argument can be generalized to n-fold wormholes.

So, the contribution of the replica wormhole saddles should be controlled by the manifold of the degenerate vacua. We have checked the above proposal in two-dimensional JT gravity and explicitly shown that the partition function of the wormhole saddle is proportional to the manifold of the twist

---

[2] The measure can be derived from the first-order formalism [35].

[3] This is similar to constrained instantons [36,37].

parameter. Furthermore, following [19–21], the wormhole geometries connecting different vacua are suggested to be regarded as the measurement process that compares different vacuum configurations. The measurement process connecting different vacuum configurations decreases the fine-grained entropy of the system, and the Page curve can also be derived by comparing the rate of the Hawking radiation and measurement processes.

For further studies, we would like to explore possible connections between the island prescription and the soft BHIP approach, which is related to the attempts to understand the BHIP using the concept of projecting black holes to specific soft hair configurations [19–21]. Especially in our recent work [20], we have started to study the possible relation between different wormhole geometries and soft hair measurements, and the disconnected Page curve shown in Fig. 7 of [20] can be regarded as transitions between different wormhole saddles. Further connections between the soft hair approach and replica wormholes might require looking closely at the black hole soft $\mathcal{S}$-matrix [38,39], which needs further study. In this triumph, the whole island prescription might be understood in terms of HPS's soft hair.

Appendix A: A review of Euclidean path integral

In this appendix, let us review and emphasize some useful concepts in QFT. This section will discuss the path integral representation of QFT and some useful concepts in black hole thermodynamics. All the selected concepts and related

interpretations will be crucial for understanding the replica wormhole later.

For a scalar field theory, the transition amplitude between $|\phi_1\rangle$ and $|\phi_2\rangle$ can be represented as the following path integral

$$\langle \phi_2(t_2)|\phi_1(t_1)\rangle = \langle \phi_2| e^{-iH(t_2-t_1)}|\phi_1\rangle = \int_{\phi(t_1)=\phi_1}^{\phi(t_2)=\phi_2} \mathcal{D}\phi\, e^{iS}. \tag{35}$$

Writing everything with Euclidean time $\tau = it$, we can express the transition amplitude as

$$\langle \phi_2(\tau)|\phi_1(0)\rangle = \langle \phi_2| e^{-\tau H}|\phi_1\rangle = \int_{\phi(0)=\phi_1}^{\phi(\tau)=\phi_2} \mathcal{D}\phi\, e^{-S_E}, \tag{36}$$

with the Euclidean action S_E. Now we have a Euclidean path integral from ϕ_1 to ϕ_2, which can be illustrated diagrammatically as follows

$$\int_{\phi(0)=\phi_1}^{\phi(\tau)=\phi_2} \mathcal{D}\phi\, e^{-S_E} = \quad \includegraphics. \tag{37}$$

The path integral is over the grey region, and ϕ_1 and ϕ_2 should serve as boundary conditions on a fixed Cauchy surface. Correspondingly, we can also express the wave function $|\Psi\rangle$ as

$$|\Psi\rangle = e^{-\tau H}|\phi_1\rangle = \int_{\phi(0)=\phi_1}^{??} \mathcal{D}\phi\, e^{-S_E} = \quad \includegraphics, \tag{38}$$

which can be measured by the overlap with state $\langle \phi_2|$ as $\Psi[\phi_2] = \langle \phi_2|\Psi\rangle$. For the wave function shown in (38), the up boundary condition is not specified. Following the same logic, the thermal density matrix ρ can be depicted as

$$\langle \phi_2| \rho |\phi_1\rangle = \langle \phi_2| e^{-\beta H}|\phi_1\rangle = \quad \includegraphics. \tag{39}$$

Taking the trace of the above density matrix gives out the thermal partition function $Z(\beta)$, which can be represented

as

$$Z(\beta) = \text{tr}\, e^{-\beta H} = \sum_{\phi} \langle \phi | e^{-\beta H} | \phi \rangle = \quad \bigcirc^{\beta} \; .$$

(40)

One can also insert some operators in the bulk to calculate correlation functions, and then (40) can be used to explain why thermal Green's function has periodicity β.

The ground state $|0\rangle$ can be got by evolving any state $|X\rangle$ for ∞ amount of time. Decomposing the state $|X\rangle$ on energy eigenstates $|n\rangle$ with $H |n\rangle = E_n |n\rangle$, the ground state can be obtained by

$$\lim_{\tau \to \infty} e^{-\tau H} |X\rangle = |0\rangle + \lim_{\tau \to \infty} \sum_{n \neq 0} e^{-\tau E_n} |n\rangle \to |0\rangle , \quad (41)$$

because all the high energy eigenstates with non-zero E_n are largely suppressed by $e^{-\tau E_n}$ as $\tau \to \infty$. The above argument can be interpreted as, after ∞-Euclidean time, all the high energy states die off, and only the vacuum state survives. Diagrammatically, we can depict the vacuum wave functional as

$$\langle \phi_2 | 0 \rangle = \int_{\phi(-\infty)}^{\phi(0)=\phi_2} \mathcal{D}\phi \, e^{-S_E} = \quad , \quad (42)$$

where the solid line labeled by $-\infty$ can be used to represent the vacuum state because only the ground state can survive after the evolution. Furthermore, it is straightforward to see that the vacuum-to-vacuum amplitude $\langle 0|0 \rangle$ can be obtained by inserting an identity

$$\langle 0|0 \rangle = \sum_{\phi} \langle 0|\phi \rangle \langle \phi|0 \rangle , \quad (43)$$

whose Euclidean path integral representation can be illustrated as

$$\langle 0|0 \rangle = \int_{\phi(-\infty)}^{\phi(\infty)} \mathcal{D}\phi \, e^{-S_E} = \quad , \quad (44)$$

where we simply glue two diagrams shown in (42) together. All the above diagrams can also be generalized to situations where ϕs are defined on boundaries with different topologies, and there can also be handles and holes in the bulk.

Next, let us consider the Rindler space and derive the Unruh effect from the Minkowski vacuum. The density matrix of the Minkowski vacuum can be written as

$$\rho = |0\rangle_M \langle 0| . \quad (45)$$

Because of the presence of the Rindler horizon, we divide the spatial surface into two parts, the $r > 0$ region A and the $r < 0$ region B. The reduced density matrix in region A can be written as

$$\rho_A = \text{tr}_B |0\rangle_M \langle 0| , \quad (46)$$

whose path integral representation is

$$\langle \phi_2 | \rho_A | \phi_1 \rangle = \sum_{\phi_B} \langle \phi_2 | \otimes \langle \phi_B | 0 \rangle_M \langle 0 | \phi_B \rangle \otimes | \phi_1 \rangle$$

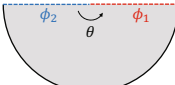$$= \sum_{\phi_B} \quad . \quad (47)$$

The trace over fields ϕ_B in region B glues the B region together. With a different foliation, the above density matrix can be depicted as

$$\sum_{\phi_B} \quad = \quad = \quad , \quad (48)$$

where the θ direction can be regarded as the Euclidean time for Rindler spacetime. So the reduced density matrix ρ_A can be regarded as a thermal density matrix with inverse temperature $\beta = 2\pi$, which can be written as

$$\langle \phi_2 | \rho_A | \phi_1 \rangle = \langle \phi_2 | e^{-2\pi H_\theta} | \phi_1 \rangle , \quad (49)$$

with the Rindler Hamiltonian H_θ. Now, we can identify the inverse temperature of Rindler space as $\beta = 2\pi$. Let us call the figure shown in equation (48) "Pacman". Now, we have derived the Unruh density matrix by tracing out the B region of the Minkowski vacuum. Besides the density matrix, the Minkowski vacuum itself can be treated from a different point of view. The vacuum wave functional measured by the overlap with state $\langle \phi_2 | \otimes \langle \phi_1 |$ can be represented as

$$\langle\phi_2|\otimes\langle\phi_1|0\rangle_M = \text{(figure)} = \langle\phi_1|\,e^{-\frac{\beta}{2}H_\theta}\,|\phi_2\rangle,$$
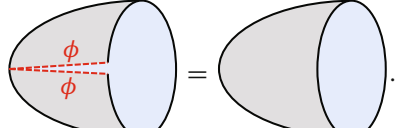
$$(50)$$

which can be further expressed as

$$\langle\phi_1|\,e^{-\frac{\beta}{2}H_\theta}\,|\phi_2\rangle = \sum_n e^{-\frac{\beta}{2}E_n}\,\langle\phi_1|n_1\rangle\otimes\langle\phi_2|n_2\rangle^*. \qquad (51)$$

$|n\rangle$ is the eigenstates of Rindler Hamiltonian H_θ on the left and right sides, with $H_\theta|n\rangle = E_n|n\rangle$. The * symbol represents the CPT transformation. Comparing (50) and (51), we can conclude that the Minkowski vacuum can be regarded as a purification of the Rindler Hilbert space

$$|0\rangle_M = \sum_n e^{-\frac{\beta}{2}H_\theta}\,|n_2\rangle^*\otimes|n_1\rangle, \qquad (52)$$

which is called thermo-field double (TFD) state [40]. We have shown the origin of the thermal spectrum for the Rindler observer restricted to the Rindler patch. The same argument can be generalized to the black hole case, which can be used to explain the thermal spectrum of the Hartle-Hawking state. The so-called "cigar" geometry replaces the disk partition function obtained from tracing the Pacman figure because of the curvature of the black hole. The black hole partition function can be represented diagrammatically as

$$Z_{BH} = \sum_\phi \text{(figure)} = \text{(figure)}. \qquad (53)$$

References

1. G. Penington, JHEP **09**, 002 (2020). https://doi.org/10.1007/JHEP09(2020)002. arXiv:1905.08255
2. A. Almheiri, N. Engelhardt, D. Marolf, H. Maxfield, JHEP **12**, 063 (2019). https://doi.org/10.1007/JHEP12(2019)063. arXiv:1905.08762v3
3. A. Almheiri, R. Mahajan, J. Maldacena, Y. Zhao, JHEP **03**, 149 (2020). https://doi.org/10.1007/JHEP03(2020)149. arXiv:1908.10996v2
4. A. Almheiri, R. Mahajan, J. Maldacena, arXiv:1910.11077v3
5. G. Penington, S.H. Shenker, D. Stanford, Z. Yang, JHEP **03**, 205 (2020). https://doi.org/10.1007/JHEP03(2022)205. arXiv:1911.11977v2
6. A. Almheiri, T. Hartman, J. Maldacena, E. Shaghoulian, A. Tajdini, JHEP **05**, 013 (2020). https://doi.org/10.1007/JHEP05(2020)013. arXiv:1911.12333v2
7. A. Almheiri, T. Hartman, J. Maldacena, E. Shaghoulian, A. Tajdini, Rev. Mod. Phys. **93**, 035002 (2021). https://doi.org/10.1007/JHEP05(2020)013. arXiv:2006.06872v1
8. D.N. Page, Phys. Rev. Lett. **71**, 3743 (1993). https://doi.org/10.1103/PhysRevLett.71.3743. arXiv:hep-th/9306083v2
9. D.N. Page, J. Cosmol. Astropart. Phys. **09**, 028 (2013). https://doi.org/10.1088/1475-7516/2013/09/028. arXiv:1301.4995v3
10. S. Ryu, T. Takayanagi, Phys. Rev. Lett. **96**, 181602 (2006). https://doi.org/10.1103/PhysRevLett.96.181602. arXiv:hep-th/0603001
11. V.E. Hubeny, M. Rangamani, T. Takayanagi, JHEP **07**, 062 (2007). https://doi.org/10.1088/1126-6708/2007/07/062. arXiv:0705.0016
12. A. Lewkowycz, J. Maldacena, JHEP **08**, 090 (2013). https://doi.org/10.1007/JHEP08(2013)090. arXiv:1304.4926
13. T. Faulkner, A. Lewkowycz, J. Maldacena, JHEP **11**, 074 (2013). https://doi.org/10.1007/JHEP11(2013)074. arXiv:1307.2892
14. T. Barrella, X. Dong, S.A. Hartnoll, V.L. Martin, JHEP **09**, 109 (2013). https://doi.org/10.1007/JHEP09(2013)109. arXiv:1306.4682
15. N. Engelhardt, A.C. Wall, JHEP **01**, 073 (2015). https://doi.org/10.1007/JHEP01(2015)073. arXiv:1408.3203
16. A.C. Wall, Class. Quantum Gravity **31**, 225007 (2014). https://doi.org/10.1088/0264-9381/31/22/225007. arXiv:1211.3494
17. H. Verlinde, arXiv:2003.13117
18. H. Verlinde, arXiv:2105.02129
19. S. Pasterski, H. Verlinde, JHEP **09**, 099 (2021). https://doi.org/10.1007/jhep09(2021)099. arXiv:2012.03850
20. P. Cheng, Y. An, Phys. Rev. D **103**, 126020 (2021). https://doi.org/10.1103/PhysRevD.103.126020. arXiv:2012.14864
21. P. Cheng, Phys. Rev. D **106**, L061904 (2021). https://doi.org/10.1103/PhysRevD.106.L061904. arXiv:2108.10177
22. S.W. Hawking, M.J. Perry, A. Strominger, Phys. Rev. Lett. **116**, 231301 (2016). https://doi.org/10.1103/PhysRevLett.116.231301. arXiv:1601.00921v1
23. S.W. Hawking, M.J. Perry, A. Strominger, JHEP **05**, 161 (2017). https://doi.org/10.1007/JHEP05(2017)161. arXiv:1611.09175v2
24. P. Cheng, P. Mao, arXiv:2211.00031
25. P. Cheng, P. Mao, Phys. Rev. D **106**, L081702 (2022). https://doi.org/10.1103/PhysRevD.106.L081702. arXiv:2206.11564
26. A. del Campo, T. Takayanagi, JHEP **02**, 170 (2020). https://doi.org/10.1007/JHEP02(2020)170. arXiv:1911.07861
27. T. Anegawa, N. Iizuka, K. Tamaoka, T. Ugajin, JHEP **03**, 214 (2021). https://doi.org/10.1007/JHEP03(2021)214. arXiv:2012.03514
28. A. Blommaert, L.V. Iliesiu, J. Kruthoff, JHEP **09**, 080 (2022). https://doi.org/10.1007/JHEP09(2022)080. arXiv:2111.07863
29. P. Saad, S.H. Shenker, D. Stanford, S. Yao, arXiv:2103.16754
30. P. Cheng, P. Mao, arXiv:2208.08456
31. A. Blommaert, L.V. Iliesiu, J. Kruthoff, JHEP **08**, 071 (2022). https://doi.org/10.1007/JHEP08(2022)071. arXiv:2203.07384
32. J. McNamara, C. Vafa, arXiv:2004.06738
33. D. Stanford, E. Witten, JHEP **10**, 008 (2017). https://doi.org/10.1007/JHEP10(2017)008. arXiv:1703.04612
34. T.G. Mertens, G.J. Turiaci, arXiv:2210.10846
35. P. Saad, S.H. Shenker, D. Stanford, arXiv:1903.11115
36. J. Cotler, K. Jensen, JHEP **11**, 070 (2022). https://doi.org/10.1007/JHEP11(2022)070. arXiv:2205.12968
37. J. Cotler, K. Jensen, Phys. Rev. D **104**, L081501 (2021). https://doi.org/10.1103/PhysRevD.104.L081501. arXiv:2010.02241
38. N. Gaddam, N. Groenenboom, arXiv:2012.02355
39. E. Himwich, S.A. Narayanan, M. Pate, N. Paul, A. Strominger, JHEP **09**, 129 (2020). https://doi.org/10.1007/JHEP09(2020)129. arXiv:2005.13433
40. J.M. Maldacena, JHEP **04**, 021 (2003). https://doi.org/10.1088/1126-6708/2003/04/021. arXiv:hep-th/0106112